

# ANALYSIS OF XFEM AND HASHIN DAMAGE TECHNIQUES CAPABILITY TO MODEL FIBRE-CEMENT BOARDS

GUSTAVO RODOVALHO BORIOLLO\* AND TULIO NOGUEIRA BITTENCOURT†

\*Escola Politécnica da Universidade de São Paulo  
São Paulo, SP Brazil  
e-mail: [gustavo.boriolo@usp.br](mailto:gustavo.boriolo@usp.br)

†Escola Politécnica da Universidade de São Paulo  
São Paulo, SP Brazil  
e-mail: [tbitten@usp.br](mailto:tbitten@usp.br)

**Key words:** Fibre-Cement, XFEM, Hashin Damage Criteria, Lightweight Facades

**Abstract:** Fibre-cement boards are commonly used on external lightweight façades for different buildings. A fibre cement material presents a pseudo strain-hardening behaviour. In addition, the post-peak is dependent of the humidity content of the material and, in traction, the material presents a multiple crack behaviour due to the interface relations between the fibres and the cementitious matrix. Understand the different mechanical behaviours of these boards, the influence of hygrometric conditions on their constitutive law and their fracture initiation and propagation criteria is important to optimize the design of facades systems. This article proposes an evaluation of the capability of the XFEM and the Hashin damage techniques implemented on ABAQUS to simulate fibre-cement boards behaviour through the 3-point bending test and the direct tensile test. Experimental results show a toughness and ductility increase with material saturation. The numerical examples indicate the capability of both techniques to capture a softening behaviour but a limitation to simulate hardening by means of fibre-bridging mechanism with the current formulations.

## 1 INTRODUCTION AND CONTEXT

Lightweight façades are a common technology used in different countries specially in Europe, North America and Asia. In Brazil, this technology has been growing slowly but the importance to implement an industrialized façade production process and their main benefits have been shown by different authors [1 - 3].

A standard lightweight façade panel typology is illustrated in Figure 1. Different materials may be adopted for the outside façade layer. Fibre-cement boards, for example, has been extensively applied as

external sheets [4,5].

To gain competitiveness and improve their benefits, a façade panel must be designed with optimized parameters. Numerical approaches, as Finite Element Analyse (FEA), are robust methods to this optimization process [6]. These methods allow a quick analysis of several configurations in order to find the most economical and confident parameters.

Having accurate numerical approximations depend on the correct input parameters of the material and a good choice of the numerical modelling technique to describe the material behaviour.

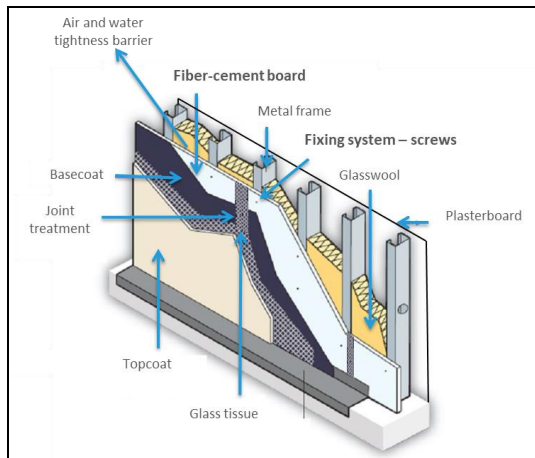


**Figure 1:** Standard lightweight façade panel typology.

In the case of a fibre-cement material, its behaviour may change within the fibre choice, fibre direction and the board production process [7]. Using synthetic fibres, as polypropylene (PP) fibres, these boards present a pseudo-strain hardening behaviour followed by a stress softening dependent of fibre debonding or fibre breakage [8]. In addition, ductility and toughness, as will be shown, are hygrometric-dependent.

Among the different criteria and techniques, the XFEM (Extended Finite Element Method) and the Hashin-based criteria deserve special attention. These techniques are widely used because of their relative easily implementation and their availability on FEA commercial softwares. Both criteria are described by some authors. Although, they have been rarely compared mainly in the case of cementitious materials [9 -12].

The objective of this paper is assess the capability and the limits of XFEM and Hashin-based techniques available in the software ABAQUS [13] in order to propose a confident approach to simulate the mechanical behaviour of a fibre-cement material.

First, the XFEM and the Hashin-based criteria techniques are compared through a concrete beam modelling with previously known results. Next, the experimental characterization of a fibre-cement board is described. Then, a comparison between the numerical techniques and the experimental results for the fibre-cement board is drawn. Finally, some conclusions are made.

## 2 XFEM AND HASHIN TECHNIQUES VALIDATION ON A CONCRETE BEAM MODELLING

Hillerborg et al. [14] were the first to propose a cohesive crack model considering the energy dissipation during the crack propagation on concrete materials. Petersson [15] uses the finite element analysis to treat numerically the fictitious crack model.

Bittencourt [16] compares what he called the Influence Method (IM), the Defined Crack Path Strategy with Interface Elements (DP) and the Arbitrary Cohesive Crack Propagation (ACC) to address cohesive crack propagation on a simply supported concrete beam in bending. For each numerical strategy, it was possible to verify their ability to detect size-dependency effects. It means, softening behaviour and a snap-back instability.

This classical exercise was chosen to validate the XFEM and Hashin techniques available in ABAQUS verifying their limits.

### 2.1 Geometry and material properties

The problem consists on a simply-supported beam under a central point load (three-point bending). The relative geometry is preserved, as shown in Figure 2, with different heights (50mm, 100mm and 300mm). Plane stress is assumed and no initial notch is considered.

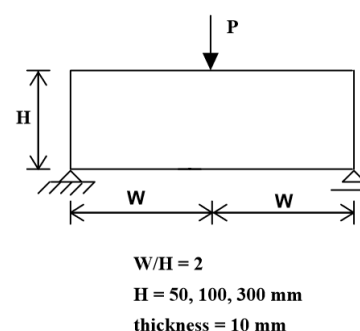


**Figure 2:** Beam geometry. Source: Bittencourt (1993).

Concrete is assumed isotropic and elastic-linear with an elastic modulus  $E = 20 \text{ GPa}$ , Poisson's coefficient  $\nu = 0.2$ , tensile strength  $\sigma_{t1} = 2 \text{ MPa}$  and energy fracture  $G_f = 0.02 \text{ N/mm}$ .

## 2.2 XFEM and Hashin modelling

### 2.2.1 Damage initiation criterion and energy fracture parameters

For both methods, it will be necessary to specify a damage initiation criterion and a damage progressive law.

The main difference between the XFEM and the Hashin approach is the damage initiation criterion: only one criterion is taken into account for the first one (maximum principal stress in this case) whereas the last one considers four damage initiation criteria (compression and tensile strength of both longitudinal (fibre) and transverse (matrix) directions) [9, 13].

In order to compare the methods, only the tensile strength was considered on the Hashin approach. All other parameters (compressive, shear and tensile strength in other directions) were assumed ten times greater than the tensile strength, as shown in Table 1. In this way, only the Mode I fracture is activated.

**Table 1:** Damage initiation and energy fracture parameters.

|                               |               |           |
|-------------------------------|---------------|-----------|
| Longitudinal tensile strength | $\sigma_{t1}$ | 2 MPa     |
| Transverse tensile strength   | $\sigma_{t2}$ | 20 MPa    |
| Compressive strength          | $\sigma_{ci}$ | 20 MPa    |
| Shear strength                | $\tau_{si}$   | 20 MPa    |
| Energy fracture               | $G_f$         | 0.02 N/mm |

### 2.2.2 Crack path dependency

Two strategies are compared: allowing a crack initiation over multiple elements and restraining cracking only in one element.

Both, XFEM and Hashin method, have presented unrealistic results if cracking is allowed on multiple elements. Figure 3 shows that multiple cracks for XFEM and a damage distribution over multiple elements for Hashin-based approach imply on a response without a softening branch and on bigger maximum load values.

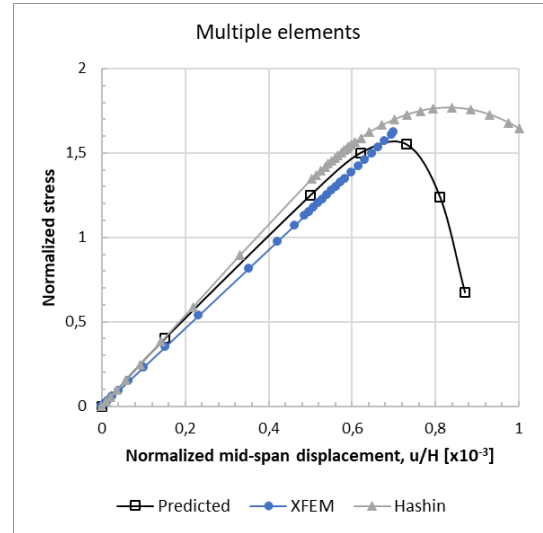


**Figure 3:** Cracking allowed on multiple elements.

## 2.3 Results comparison

The analysis made by Bittencourt [16] illustrates the size-dependency of the concrete response. Through the Influence Method, it can be accurately observed the changing on the stress-displacement curves with the different beam heights.

The same problem presented in 2.1 was treated using the modelling parameters detailed in 2.2. From Figures 4, 5 and 6 it has been observed a comparison between XFEM, Hashin, IM and DP results for different beam heights.

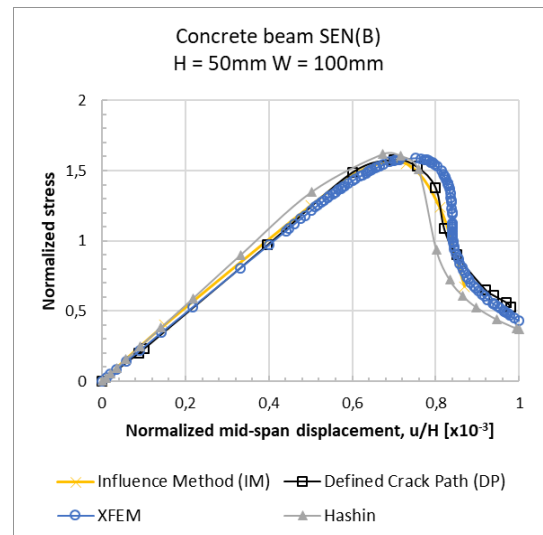


**Figure 4:** Stress-displacement curves comparison. H = 50mm and W = 100mm.

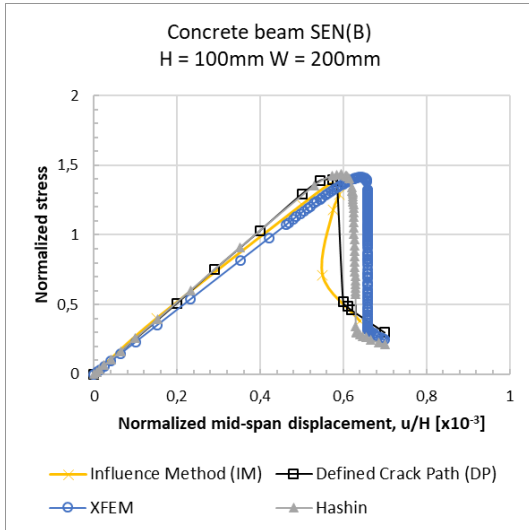


**Figure 5:** Stress-displacement curves comparison.  $H = 100\text{mm}$  and  $W = 200\text{mm}$ .

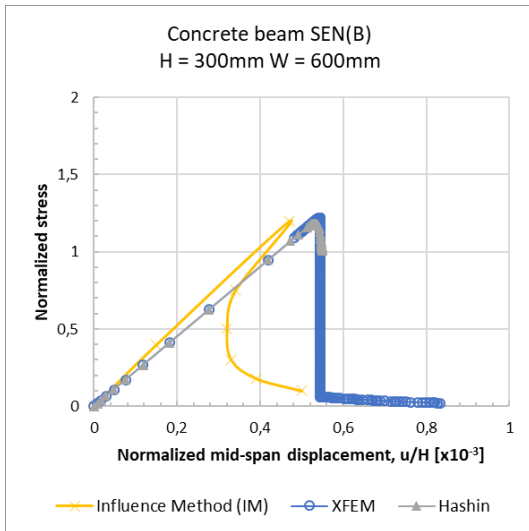


**Figure 6:** Stress-displacement curves comparison.  $H = 300\text{mm}$  and  $W = 600\text{mm}$ .

The normalized stress, as defined by Bittencourt, is the ratio between the beam

theory maximum tensile stress for the uncracked beam at midspan and the longitudinal tensile strength.

Table 2 summarizes the results in terms of maximum load and energy, calculated as the area under the load-displacement curve.

It can be seen that both XFEM and Hashin method give a good approximation of the maximum load prediction. The XFEM results has an approximation of about +3% in relation with the IM technique, and of about +1% compared to the DP method. For Hashin results, maximum load prediction is around 5% higher than the IM values and around 3% higher than the DP results.

XFEM and Hashin method show a good agreement along the softening path for the smallest beam (Figure 4). As the DP method, neither XFEM nor Hashin technique are able to capture the snap-back behaviour, as illustrated in Figures 5 and 6. However, for both methods there is a sudden-jump in these curves with a good agreement with the other portions of the curves, including the softening branch at the end. The snap-back instability, in turn, may not be physically feasible.

### 3 EXPERIMENTAL CHARACTERIZATION OF THE FIBRE-CEMENT BOARD

Two experimental tests were done in order to characterize the fibre-cement material behaviour: the three-point bending test and the direct tensile test.

**Table 2:** Maximum load and Energy obtained by different numerical methods.

| H / W                     | 50 / 100       |               | 100 / 200      |               | 300 / 600      |               |
|---------------------------|----------------|---------------|----------------|---------------|----------------|---------------|
|                           | $P_{\max}$ (N) | Energy (N.mm) | $P_{\max}$ (N) | Energy (N.mm) | $P_{\max}$ (N) | Energy (N.mm) |
| <b>Influence Method</b>   | 129,2          | 3,42          | 228,3          | 7,29          | 200,0          | 3,01          |
| <b>Defined Crack Path</b> | 131,7          | 3,70          | 232,5          | 8,20          | -              | -             |
| <b>XFEM</b>               | 132,7          | 3,76          | 235,5          | 8,49          | 203,4          | 5,75          |
| <b>Hashin</b>             | 134,7          | 3,72          | 239,5          | 8,27          | 197,2          | 5,67          |

The cementitious material with short polypropylene and cellulose fibres was tested after different conditioning states:

- Ambient condition: laboratory ambient conditions (23 °C and 50% RH);
- Wet condition: immersion in water at ambient temperature;
- Dry condition: drying in a ventilated oven at 100 °C.

In all cases, the tests were carried out after mass stabilization on the correspondent conditioning process.

### 3.1 Three-point bending test

The three-point bending test was performed following the methodology described by the Brazilian standard for fibre-cement products without asbestos – NBR 15498:2016 [17]. This methodology is used to the quality control of the production. Therefore, the main objective is understanding how the parameters obtained by the test may help the numerical strategy to simulate the material.

As the material is orthotropic in plane [7], all boards were tested on the longitudinal direction, it means, the fibres are subjected to traction loads due to the bending. The test set-up is illustrated in Figure 7.

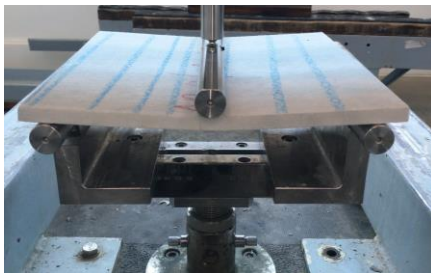


**Figure 7:** Test apparatus and sample positioning for the three-point bending test.

Five samples of 250mm x 250mm x 10mm for each conditioning state were tested. Figure 8 presents the average load-displacement curve for all conditions.

It can be seen that the hygrometric conditions have an important influence on the material strength and on the softening behaviour (post-peak). The elastic behaviour has not a significant changing whatever the

hygrometric condition.

In terms of fracture modelling, the main differences observed are the damage initiation point – changing the material strength – and the fracture energy – related to the total energy absorbed by the specimen (area under the load-displacement curve).

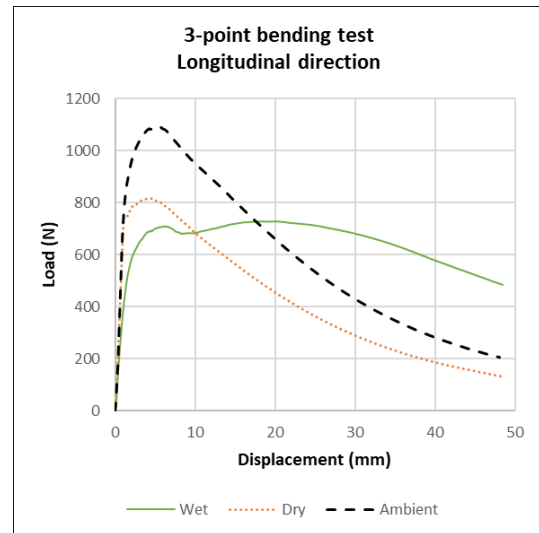


**Figure 8:** Load-displacement curve for the three-point bending test in different hygrometric conditions.

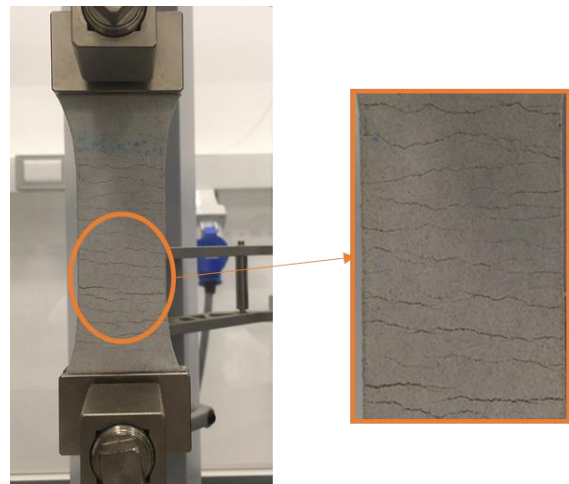


**Figure 9:** Multiple fissures due to fibre-bridging in the direct tensile test.

### 3.2 Direct tensile test

The objective of this test is observing the fibre-cement cracking behaviour. With the material subjected to direct traction, the fibre-bridging mechanism is marked and the different failure stages (matrix cracking, fibre-bridging and fibre pull-out) are highlighted [18].

The experimental methodology was adapted to the ASTM D1037-12 for wood-based fibre panels [19]. Testing were performed in a universal testing machine Shimadzu AGS-X with a controlled displacement rate of 0,5 mm/min. Three samples were analysed in wet and in ambient conditions.

By looking at Figure 9 it can be noted a multi cracking process. As described by Li [8], after the first macro crack bridging fibres redistribute the load back to the matrix via fibre/matrix interface, charging other matrix points until attaining their maximum strength.

Figure 10 shows that the material strength decreases with its saturation. On the other hand, material toughness is increased in saturated condition and fibre-bridging effect is increased. The end of the linear region represents the matrix strength. After the elastic phase, first crack appears but the material stays withstanding the load by the fibre-matrix interaction. In the wet condition, maximum load is attained after an important fibre elongation and this value is much greater than the matrix strength.

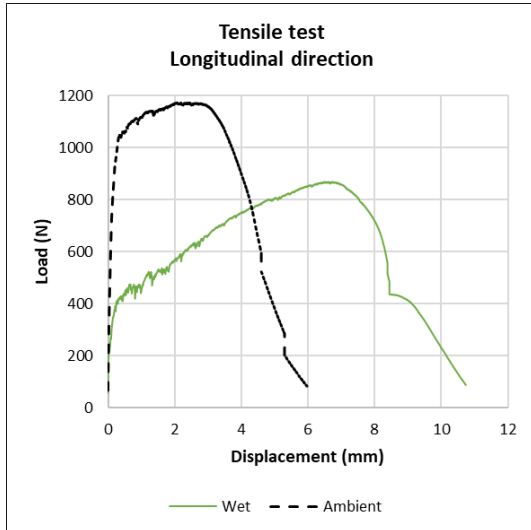


**Figure 10:** Load-displacement curves for the direct tensile test in different hygrometric conditions.

#### 4 NUMERICAL MODELLING OF THE FIBRE-CEMENT BOARD

The numerical models were made using the software ABAQUS v6.14-6. Both tests presented in Section 3 were modelled using

the XFEM and the Hashin technique. 2D models are proposed assuming plane stress. The specimens were meshed with quadrilateral elements. The element used was the CPS4, an ABAQUS element for 2D solid sections with a plane stress formulation, four integration nodes and a bilinear interpolation function [13].

As showed in Section 2, the specimens were modelled with cracking allowed only in their central element.

Elastic properties were obtained by the experimental material characterization. The elastic modulus is not the same if obtained by the bending test or by the direct tensile test. Table 3 summarizes the Young's modulus measured in the different conditions. Poisson's coefficient is assumed 0,21.

**Table 3:** Elastic moduli in different test conditions.

|                | <b>3-point bending test</b> | <b>Direct tensile test</b> |
|----------------|-----------------------------|----------------------------|
| <b>Ambient</b> | 7,9 +/- 0,6 GPa             | 1,9 +/- 0,2 GPa            |
| <b>Wet</b>     | 7,5 +/- 0,9 GPa             | 1,8 +/- 0,3 GPa            |
| <b>Dry</b>     | 7,1 +/- 0,4 GPa             | -                          |

Through the numerical simulation with FEA, the damage initiation and the energy fracture were defined for each condition fitting the numerical results to the experimental curves.

##### 4.1 Three-point bending test

The three-point bending test was simulated in two-dimensions by a rectangular simply supported beam with a 215mm span and 10mm height, as shown in Figure 11. The supports were represented by two nodes restrained on the vertical displacement.

Crosshead displacement was represented by a progressive displacement applied on the top of the beam at midspan. The applied displacement was considered distributed on 1mm to avoid stress concentration under a unique displacement application point.



**Figure 11:** Boundary conditions

Figures 12, 13 and 14 show that XFEM and Hashin simulations present a good agreement with experimental results on the linear elastic behaviour whatever the hygrometric content. On the other hand, the non-elastic behaviour prediction is not properly fitted for all testing conditions.

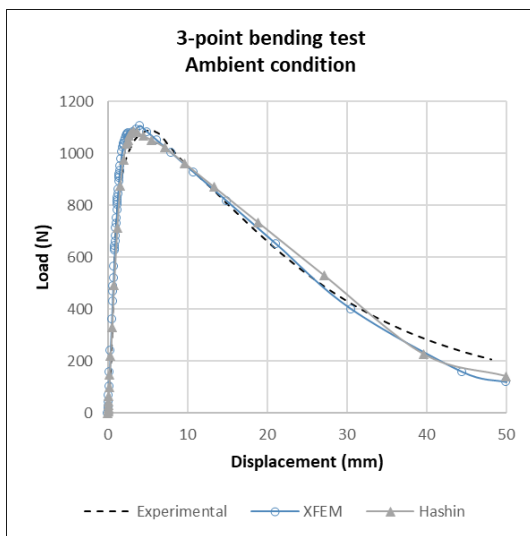


**Figure 12:** Load-displacement simulated response in ambient condition.

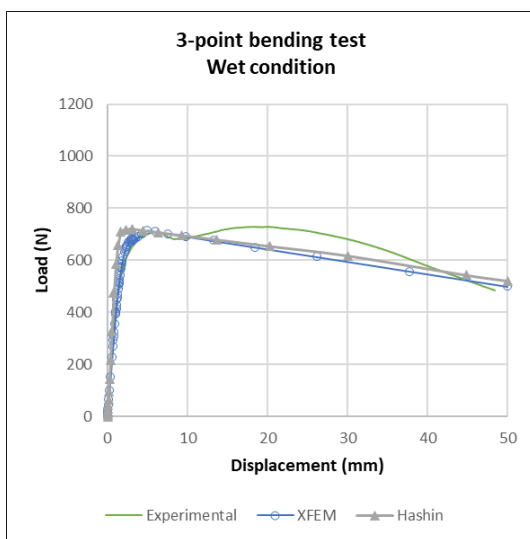


**Figure 13:** Load-displacement simulated response in wet condition.

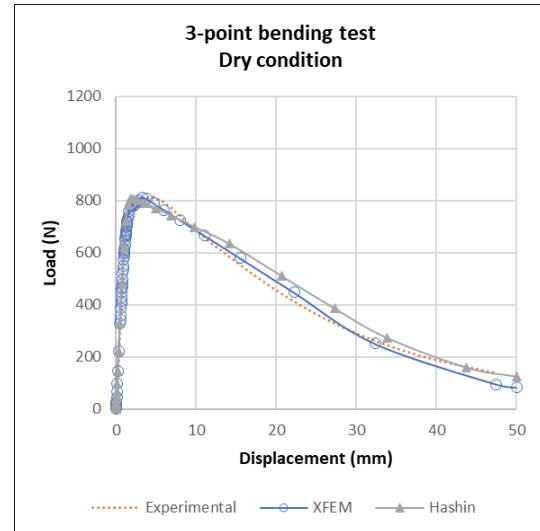


**Figure 14:** Load-displacement simulated response in dry condition.

When the material presents a stress softening behaviour after the first peak load, it can be noted that numerical results estimate appropriately the maximum load and the post-peak behaviour. It is the case of the mechanical behaviour in ambient and in dry condition.

In wet condition, the fibre-cement tested shows a quite hardening behaviour after the first peak load. In this situation, neither XFEM nor Hashin are able to capture the hardening effect on the material. In both numerical methods, the degradation process is uniform and irreversible after the damage initiation.

In each hygrometric condition, a sensibility analysis was made in order to understand how the variability of the fracture parameters influences on the material load-displacement predicted response. Damage initiation criterion was adopted as the maximum principal stress and the fracture propagation law is the energy-based law available in ABAQUS. Stress strength ( $\sigma_i$ ) and energy fracture ( $G_f$ ) were defined in Table 4 in order to the relative error

in maximum load and energy prediction was less than 2% for all conditioning states. Table 5 summarizes the maximum load predicted

and the energy calculated in each hygrometric configuration.

**Table 4:** Fracture parameters defined to numerical simulations.

| Conditioning  | Ambient             |                 | Wet                 |                 | Dry                 |                 |
|---------------|---------------------|-----------------|---------------------|-----------------|---------------------|-----------------|
|               | $\sigma_i$<br>(MPa) | $G_f$<br>(N/mm) | $\sigma_i$<br>(MPa) | $G_f$<br>(N/mm) | $\sigma_i$<br>(MPa) | $G_f$<br>(N/mm) |
| <b>XFEM</b>   | 5,6                 | 16,5            | 3,5                 | 35,0            | 4,1                 | 12,0            |
| <b>Hashin</b> | 5,8                 | 14,0            | 4,0                 | 32,0            | 4,7                 | 11,0            |

**Table 5:** Maximum load and energy predicted by numerical simulations.

| Conditioning        | Ambient          |                  | Wet              |                  | Dry              |                  |
|---------------------|------------------|------------------|------------------|------------------|------------------|------------------|
|                     | $P_{max}$<br>(N) | Energy<br>(N.mm) | $P_{max}$<br>(N) | Energy<br>(N.mm) | $P_{max}$<br>(N) | Energy<br>(N.mm) |
| <b>Experimental</b> | 1091,9           | 28437            | 726,9            | 31178            | 815,6            | 20299            |
| <b>XFEM</b>         | 1105,7           | 28051            | 713,4            | 30996            | 812,1            | 20392            |
| <b>Hashin</b>       | 1086,6           | 28728            | 718,2            | 31083            | 808,0            | 21764            |

It is clear that there is a slightly difference between the XFEM fracture strategy and the Hashin damage model in ABAQUS. For Hashin model it is important to emphasise that the damage initiation and the cracking progress is dependent of a more complete characterization of longitudinal and transverse material tensile and compression strength.

However, even with quite different parameters, both methods are able to capture the material mechanical behaviour properly if strain hardening is not present.

#### 4.2 Direct tensile test

To simulate the direct tensile test, the specimen was modelled in 2D as shown in Figure 15. Vertical displacements are restrained at the bottom region and a progressive displacement was applied at the top region of the geometry.

Hardening effect and fibre-bridging effect are really marked on this test, as showed in 3.2. The numerical strategies with XFEM or Hashin formulation are not capable to depict these non-linear effects as observed in Figure 16. Only the ambient condition is presented, but the results are the same in the wet condition.

To get best results for this behaviour a properly description of the fibre-matrix

interaction is necessary. The models must be improved with fibre-bridging formulation laws to be able to describe the forces fibres exert on crack faces [20, 21]. A model in more fine scale or a strategy to add fibre-bridge energy consumption in the current formulation will be proposed in future researches.

#### 5. CONCLUDING REMARKS

XFEM and Hashin damage model were used to simulate the fracture behaviour of a concrete beam and of a fibre-cement board.

The expected behaviour of the concrete beam was taken into the literature. For the fibre cement material, an experimental characterization program was conducted.



**Figure 15:** Geometry and boundary conditions to the direct tensile test.



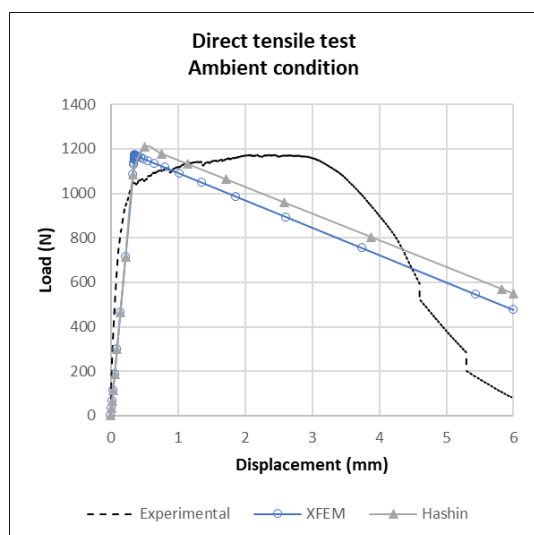


**Figure 16:** Load-displacement curve for direct tensile test numerical simulations in ambient condition.

Observing the numerical and the experimental results, some conclusions are drawn:

- Fibre-cement with polypropylene and cellulose fibres presents a hygrometric dependent mechanical behaviour;
- XFEM and Hashin method provide a good description of the linear elastic behaviour of the material both for the concrete and the fibre-cement analysis;
- The non-linear behaviour prediction does not always have a good agreement. Softening behaviour is well captured. However, neither the snap-back effect on the concrete beam nor the hardening and fibre-bridging behaviour on the fibre-cement board were properly detected;
- The input parameters for XFEM progressive cracking are only the maximum material strength and a homogenised fracture energy. Hashin model needs a more detailed material description with fibre and matrix strength in different directions. Experimental characterization of all these parameters is not evident. In contrast, Hashin model provides a

more realistic material description for orthotropic materials;

- In order to predict hardening and fibre-bridging behaviour correctly, it is necessary a more detailed model. The model needs to take into account the fibre-matrix interaction energy and the constitutive law must be defined as a hygrometric-dependent law.

## 6. ACKNOWLEDGEMENTS

The authors wish to acknowledge the technical and financial support of Saint-Gobain Research Brasil. This research is also financially supported by the French Embassy in Brazil through the “*Docteurs en Entreprise*” program.

## 7. REFERENCES

- [1] Steel Construction Institute, 2008. Best practice in steel construction residential buildings. Ascot: SCI.
- [2] Barros, M.M., and Sabbatini, F.H., 2003. Diretrizes para o processo de projeto para a implantação de tecnologias construtivas racionalizadas na produção de edifícios. *Boletim Técnico BT/PCC/172*, São Paulo; p.24.
- [3] Olivieri, H., et al., 2017. Adopting new construction systems to reduce the use of resources in constructions sites: Light Steel Framing. *Ambiente Construído*. **17(4)**: pp.45-60.
- [4] Cardoso, S.S., 2016. Tecnologia construtiva de fachada em chapas delgadas estruturadas em light steel framing. Master dissertation, Universidade de São Paulo. São Paulo.
- [5] Santiago, A.K. et al., 2012. Steel framing: arquitetura. *Manual técnico*. Instituto Aço Brasil. Rio de Janeiro.
- [6] Wang, X. et al., 2018. Finite element analysis and lightweight optimization

- design on main frame structure of large electrostatic precipitator. *Advances in Materials Science and Engineering*. **2018**: pp.1-11.
- [7] Bentur, A., and Mindess, S., 2007. *Fibre reinforced cementitious composites*. 2<sup>nd</sup> ed. CRC Press.
- [8] Li, V.C, and Wang, H.C, 1992. Pseudo strain-hardening design in cementitious composites; *Proc. Of International Workshop on High Performance Fiber Reinforced Cement Composites*, Ed. H. Reinhardt and A. Naaman, Chapman and Hall: pp. 371-387.
- [9] Duarte, A.P.C. et al., 2017. Comparative study between XFEM and Hashin damage criterion applied to failure of composites. *Thin-Walled Structures*. **115**: pp. 277-288.
- [10] Li, S., and Sitnikova, E., 2018. A critical review on the rationality of popular failure criteria for composites. *Composites Communications*. **8**: pp. 7-13.
- [11] Gu, J. and Chen, P., 2017. Some modifications of Hashin's failure criteria for unidirectional composite materials. *Composite Structures*. **182**: 143-152.
- [12] Huang, Y., et al., 2018. Characterization of mortar fracture based on three-point bending test and XFEM. *Int. J. of Pavement Research and Technology*. **11**: 339-344.
- [13] Dassault Systèmes. ABAQUS Analysis User's Manual v.6-14. Providence, USA. 2014.
- [14] Hillerborg, A. et al., 1976. Analysis of crack formation and crack growth in concrete by means of fracture mechanics and finite elements. *Cement and Concrete Research*. **6**: pp. 773-782.
- [15] Petersson, P-E., 1981. Crack growth and development of fracture zones in plain concrete and similar materials. *Report TVBM-1006/1-174*, Division of Building Materials, Lund Institute of Technology. Lund, Sweden.
- [16] Bittencourt, T.N., 1993. Computer simulation of linear and nonlinear crack propagation in cementitious materials. *Doctoral thesis*. Cornell University. Ithaca, USA.
- [17] Associação Brasileira de Normas Técnicas, 2016. Non-asbestos fibre-cement flat sheets – Specification and test methods. NBR 15498. *Brazilian standards*. Rio de Janeiro: ABNT.
- [18] Noushini, A. et al., 2013. Flexural toughness and ductility characteristics of polyvinyl-alcohol fibre reinforced concrete (PVA-FRC). In Van Mier et al. (eds). *Proc. of VIII Int. Conf. on Fract. Mech. of Conc. and Conc. Struc. (FraMCoS-8)*. March 10-14, 2016, Toledo, Spain.
- [19] ASTM Standard D1037, 2012. Standard test methods for evaluating properties of wood-base fiber and particle panel materials. ASTM International, West Conshohocken, PA.
- [20] Afshar, A. et al., 2015. XFEM analysis of fiber bridging in mixed-mode crack propagation in composites. *Composite Structures*. **125**: pp. 314-327.
- [21] Wang, H.W. et al., 2014. Application of extended finite element method in damage progress simulation of fiber reinforced composites. *Materials and Design*. **55**: pp. 191-196.